MIMO Capacity Variation with SNR and Multipath Richness from Full-wave Indoor FDTD Simulations *

*Jon W. Wallace and Michael A. Jensen

Department of Electrical and Computer Engineering,
459 CB, Brigham Young University, Provo, UT 84602-4099,
wall@ieee.org, jensen@ee.byu.edu

1 Introduction

Information theoretic studies show that multiple-input multiple-output (MIMO) wireless systems can achieve very high spectral efficiencies for single-user communication [1, 2]. For a fixed average receive SNR, the capacity of a MIMO system is directly proportional to the available multipath, implying that high multipath is actually a desirable characteristic for a communications channel. Intuition suggests, however, that scattering phenomena leading to strong multipath also introduce high pathloss (low average receive SNR). Therefore, one might expect high SNR and high multipath to be competing goals. Ultimately, we may wish to know what characteristics are important for a "good" or high capacity channel. Such knowledge specifies what environments will truly benefit from MIMO architectures and allows optimal planning and deployment of MIMO systems.

In this work, we demonstrate the joint effect of pathloss and multipath richness on capacity through two-dimensional (2D) finite-difference time-domain (FDTD) simulations [3]. The scenario under study is a simplified model of a section of the 4th floor of the engineering building on the Brigham Young University campus. We find that multipath richness is fairly constant, and that the capacity is mostly a function of the pathloss. A capacity multiplier analysis shows that when average SNR in the environment is high, MIMO systems tend to be very advantageous. However, when average SNR is low, most of the advantage of the multiple antennas comes from diversity and not spatial multiplexing.

2 FDTD Simulations

The FDTD method was chosen for ease of implementation and its ability to capture all important scattering mechanisms. Two-dimensional simulations were necessary to allow simulation of a sufficiently large area. Limiting simulations to 2D essentially reduces the pathloss exponent, which we feel is acceptable for the goals of the study.

Figure 1 depicts the FDTD simulation area, where only the cinder block walls (homogeneous dielectric with $\epsilon_r = 2$) and supporting beams (solid perfect conductors) were included. An excitation of 2.45 GHz was assumed and the region was discretized at a spatial resolution of 8 cells per wavelength.

Separate simulations were run for 9 different transmit antenna positions located along a uniform linear array (ULA) with $\lambda/2$ inter-element spacing, where λ is the free-space wavelength. The excitation signal was a $\hat{z}$-directed (vertical) current source driven with a sine wave. Simulations were run for 400 sinusoidal periods in order to reach steady-state operation. The time-domain E_z field component was stored on a $\lambda/2$-spaced grid over the entire simulation domain for the last simulation period. The response at the center frequency was then obtained from an FFT.

*This work was supported by the National Science Foundation under Wireless Initiative Grant CCR 99-79452 and Information Technology Research Grant CCR-0081476.

Fairly arbitrary receive arrays could be formed from the stored data. Here, a 4×4 uniform rectangular array with $\lambda/2$ inter-element spacing was chosen. Receive arrays were synthesized at sample points lying on a Cartesian grid over the complete floor plan with a grid spacing of 5λ. Sample points that were inside walls or within 10λ of the center transmit antenna were discarded, leaving 1894 remaining points. The channel transfer response from the jth transmit antenna to the ith receive antenna for the sth receive array position is $h_{i,j,s}$. The $N_R = 16$ transmit by $N_T = 9$ receive channel matrix for position s is $\mathbf{H}_s$.

3 SNR, Multipath Richness, and Capacity

In this study, relative SNR at location s is defined as

$$\mathrm{SNR}_{\mathrm{rel}}^{(s)} = \frac{1}{N_T N_R \, A} \sum_{i,j} |H_{i,j,s}|^2, \quad A = \frac{1}{N_T N_R N_S} \sum_{i,j,s} |H_{i,j,s}|^2, \tag{1}$$

where $N_S = 1894$ is the number of receive array locations. Figure 2 shows the relative receive SNR for all positions. Apparent in the plot is the wave guiding of the hallway, significant propagation through walls, and shadowing due to metal beams.

Multipath richness has been quantified using the effective degrees of freedom (EDOF) metric [4]. We use an alternative SNR-independent definition of EDOF for a single channel realization as $\mathrm{EDOF} = \sum_k S_k / \max_k S_k$, where S_k is the kth singular value of the channel matrix. This value lies on the range $[1, \min(N_T, N_R)]$ and represents the effective number of parallel channels that can be formed.

Capacity is computed using the water-filling solution [2], with each receive antenna having a constant (complex) noise variance of $\sigma^2 = \mathrm{SNR}_{\mathrm{ref}} A$, where $\mathrm{SNR}_{\mathrm{ref}}$ is a convenient *reference* SNR. Setting the reference SNR has the effect of shifting the scale in Figure 2 by the reference value.

Figure 3 plots the capacity, relative SNR, and EDOF as a function of the separation of the transmitter and receiver for a reference SNR of 20 dB. As one would expect, the SNR and multipath richness decrease and increase, respectively, with increasing separation distance. The capacity is more strongly affected by the SNR variation than EDOF variation. Also, we see that the EDOF parameter changes only modestly over the range of distances. Therefore, in this scenario, increasing separation distance is not advantageous, since the slight increase in multipath cannot compensate for lost receive SNR.

Figure 4 plots the approximate functional relationship between the three important parameters of capacity, relative SNR, and EDOF. Although average capacity is strongly affected by SNR, it is only weakly affected by the EDOF parameter. Also, we see the expected inverse dependence of SNR and EDOF.

4 Capacity Multiplier Analysis

Simulations and measurements confirm that MIMO systems offer a large capacity increase over single antenna systems. However, is full spatial multiplexing usually required to obtain this improvement? In this study we analyze the data for three possible systems: (1) single-transmit single-receive (SISO), (2) optimal transmit/receive diversity (equivalent to maximum ratio transmission [5]), and (3) complete spatial multiplexing (MIMO). In each case a channel capacity can be computed under the constraints of the signaling system to obtain C_{SISO}, C_{DIV}, and C_{MIMO}, respectively.

Since C_{SISO} only varies according to the relative SNR, we will consider C_{SISO} as the baseline capacity. Next, we define the multiplier $M_{\mathrm{D}} = C_{\mathrm{DIV}}/C_{\mathrm{SISO}}$, which quantifies capacity improvement due to diversity. This improvement will depend on the spatial distribution of the multipath and how much power gain can be extracted through proper weighting. Finally, we define $M_{\mathrm{M}} = C_{\mathrm{MIMO}}/C_{\mathrm{DIV}}$, which quantifies the capacity increase from spatial multiplexing and is proportional to the richness of the multipath. Studies on the i.i.d. Gaussian channel suggest that for very rich multipath, $M_{\mathrm{D}}M_{\mathrm{M}} = \min(N_T, N_R)$. Our multiplier analysis shows how close we are to the ideal i.i.d. Gaussian channel and indicates the reason for the capacity increase. In the following, we consider both high (20 dB) and low (0 dB) reference SNRs.

Plots for C_{SISO} (not shown) look very similar to Figure 2, since capacity is essentially just the logarithm of power. Figure 5 plots the two multipliers for the high reference SNR. Although M_{D} is highest in the shadow regions, it is fairly constant throughout the simulation area. The multiplexing multiplier M_{M} can actually be high very near the transmitter, demonstrating that high SNR and high multipath are not necessarily mutually exclusive. Figure 6 plots cdfs of the base capacity and multipliers. The capacity increase afforded by MIMO is large, and both diversity and multiplexing play a major role in the capacity increase.

In the case of a low reference SNR (0 dB), the multiplier plots look very similar to Figure 5, except that the range on M_{D} is much larger, and the range on M_{M} is shifted down. Figure 7 plots cdfs for this low SNR case. Again, a substantial improvement in capacity is afforded by the MIMO system. However, most of the improvement comes from diversity and not spatial multiplexing.

5 Conclusion

We have presented full-wave FDTD simulations of an indoor environment and studied the relationship of SNR, EDOF, and capacity. Capacity varies most notably with respect to the relative SNR. The multipath richness, quantified by EDOF, varies only weakly in the environment. A capacity multiplier analysis demonstrated that for high SNR, MIMO systems are very advantageous throughout the indoor channel, and that for low SNR most of the improvement can be captured by simple diversity techniques.

References

[1] G. J. Foschini and M. J. Gans, "On limits of wireless communications in a fading environment when using multiple antennas," *Wireless Personal Communications*, vol. 6, pp. 311–335, Mar. 1998.

[2] G. G. Raleigh and J. M. Cioffi, "Spatio-temporal coding for wireless communication," *IEEE Transactions on Communications*, vol. 46, pp. 357–366, Mar. 1998.

[3] A. Taflove, *Computational Electrodynamics: The Finite Difference Time Domain Method*. Artech House, 1995.

[4] D.-S. Shiu, G. J. Foschini, M. J. Gans, and J. M. Kahn, "Fading correlation and its effect on the capacity of multielement antenna systems," *IEEE Transactions on Communications*, vol. 48, pp. 502–513, Mar. 2000.

[5] T. K. Y. Lo, "Maximum ratio transmission," in *IEEE ICC'99*, vol. 2, (Vancouver, BC, Canada), pp. 1310–1314, June 6-10 1999.

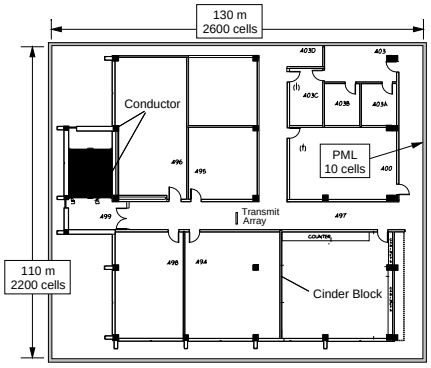

Figure 1: FDTD simulation area

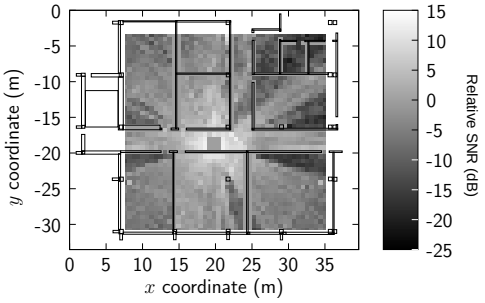

Figure 2: Relative SNR vs receive position

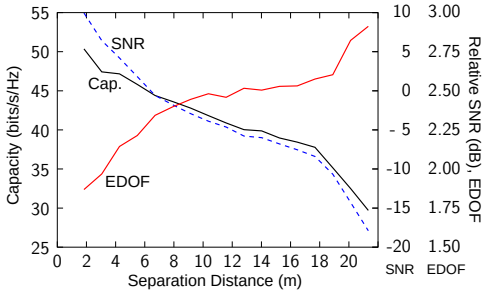

Figure 3: Relative SNR, EDOF, and capacity vs. transmit/receive separation distance

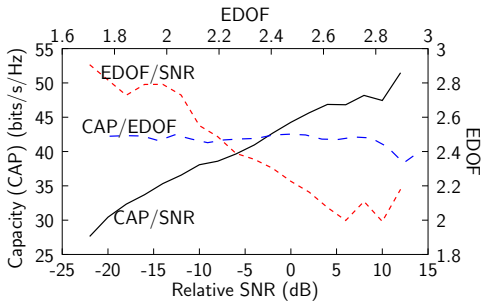

Figure 4: Empirical functional relationship of relative SNR, EDOF, and capacity

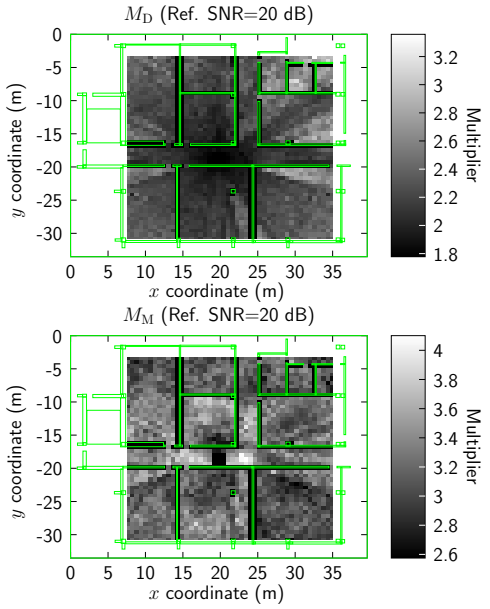

Figure 5: Diversity and multiplexing capacity multipliers for a reference SNR of 20 dB

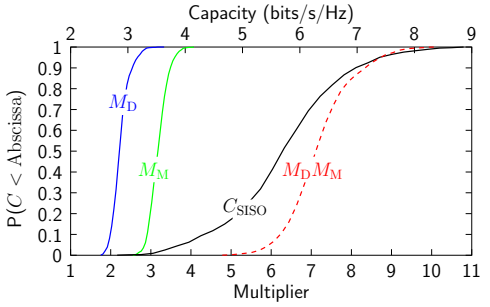

Figure 6: SISO capacity and capacity multiplier cdfs for a reference SNR of 20 dB

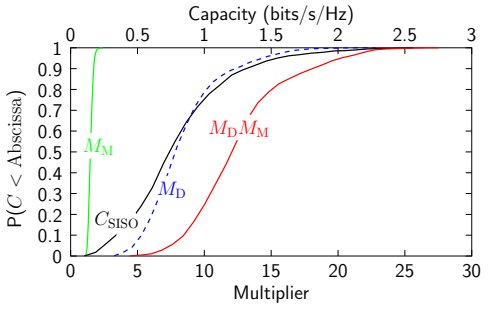

Figure 7: SISO capacity and capacity multiplier cdfs for a reference SNR of 0 dB